Proceedings World Geothermal Congress 2020+1
Reykjavik, Iceland, April - October 2021

Fault-controlled Fluid Flow in Fractured Geothermal Systems: Structural Control on the Development of the Liquiñe Geothermal Area, Southern Volcanic Zone of the Andes (39ºS)

Gloria Arancibia[1,2,*], Tomás Roquer[1,2], Julie Rowland[3], E. Andrés Veloso[1,2], Eduardo Molina[1,2], Josefa Sepúlveda[1,2], Jorge Crempien[1,2], Diego Morata[2,4]

1. Departamento de Ingeniería Estructural y Geotécnica, Pontificia Universidad Católica de Chile, Santiago, Chile
2. Centro de Excelencia en Geotermia de los Andes (CEGA - FONDAP), Universidad de Chile, Santiago, Chile
3. The University of Auckland, School of Environment, Auckland, New Zealand
4. Departamento de Geología, Universidad de Chile, Santiago, Chile

garancibia@ing.puc.cl

Keywords: Fault Zones and Fluid Flow; Liquiñe-Ofqui Fault System; Andean Transverse Faults

ABSTRACT

Fault zones and fracture networks control the spatial distribution and development of fluid flow in the upper crust, by acting by conduit or barriers for crustal fluid flow (e.g. magma and groundwater flow). The nature of long and short-term geological conditions for fluid flow in fault zones, is critical to know the tectono-hydraulic behavior on natural fractured systems. We propose the Southern Volcanic Zone (Southern Andes, Chile) as a case study to evaluate the role of the structural permeability in primarily low porosity crystalline rocks of the North Patagonian Batholith. Recently published work propose a relatively well-constrained first-order role of two active fault systems in fluid flow at crustal scales: the arc-parallel (NNE-striking) Liquiñe Ofqui Fault System (LOFS) and the arc-oblique (NW to WNW-striking) Andean Transverse Faults (ATF). Such role depends on the elastic response of the intra-arc in the different phases of the Andean Seismic Cycle. The LOFS is composed of active NNE-striking dextral and dextral-reverse master faults, favorably oriented for vertical fluid flow during long-term stress conditions (Andean interseismic). The ATF include a group of NW to WNW-striking morphotectonic lineaments, and sinistral and sinistral-reverse faults associated with long-lived discontinuities of the Andean basement. The ATF is unfavorably oriented for vertical fluid flow in the long-term stress conditions and would therefore favors the storage of hydrothermal fluids. However, vertical fluid flow would be enhanced at short-term stress conditions for this fault system (Andean co- and postseismic). Preliminary results indicate the occurrence of low-to-medium enthalpy geothermal system, where natural hot springs upwelling from fractured granite or from fluvial deposits overlying granitoids, spatially related to regional mapped faults and morphotectonic lineaments of the faults governing regional tectonics (LOFS and ATF). We now propose to examine the Liquiñe (~39°S) area as a site of interaction between these fault systems, in order to evaluate the naturally fractured geothermal system. We collected and inverted fault-slip data in 2 selected structural sites, Los Añiques (n=70) and Cachim, (n=44), to propose long-term strain tectonic solutions. Each of the studied sites shows 2 tectonic solutions of strain that essentially interchange the orientations of the shortening (P) and extension axes (T) keeping the intermediate axis vertical, compatible with strike-slip regime. In Los Añiques, Solution I has P=240/04 and T=330/25, whereas Solution II has P=300/17 and T=210/02. In Cachim Solution I has P=260/01 and T=170/14, whereas Solution II has P=175/21 and T=265/05. Solution I is kinematically coupled with long-term stress conditions, whereas solution II seems to be decoupled and it is therefore likely related to local and/or sporadic stress perturbations (e.g. Andean Seismic Cycle). Our results confirm that tectono-hydraulic behavior of the geothermal system of Liquiñe is controlled by varying kinematic conditions, rather than by homogeneous strain.

1.INTRODUCTION

Fault zones can control the location, emplacement, and evolution of economic mineral deposits and geothermal systems related to fluid circulation in the crust (e.g. Cox et al., 2001; Sibson, 2001; Caine et al., 2010; Micklethwaite et al., 2010). From the point of view of the architecture and hydromechanical properties in the upper crust, a fault zone consists of a fault core (single or multiple) where deformation is concentrated and a damage zone consisting of widely fractured whole rock (Fig. 1a). Structural permeability is given by secondary fracture networking that can improve significantly the fluid flow in the fault core and damage zone, enhancing the hydraulic conductivity of the fault zone respect to the intrinsic (or primary) permeability of country rocks (Fig. 1b) (e.g. Faulkner et al., 2010; Seebeck et al., 2014).

Additionally, in tectonically active regions, the geometry and internal structure of fault/fractures and vein networks are controlled by fault-valve and pumping behavior (e.g. Sibson, 2001; Cox, 2010). Such abrupt fluctuations in fluid pressure are linked to the earthquake cycle during interseismic period and they are particularly likely in faults that being unfavorably oriented for frictional reactivation in prevailing stress fields. Therefore, the conduit/barrier behavior of fault zones has widely been documented in the literature as “structural control on crustal fluid flow” (e.g., Cox et al., 2001; Rowland and Sibson, 2004; Micklethwaite et al., 2010; Gudmundsson, 2011).

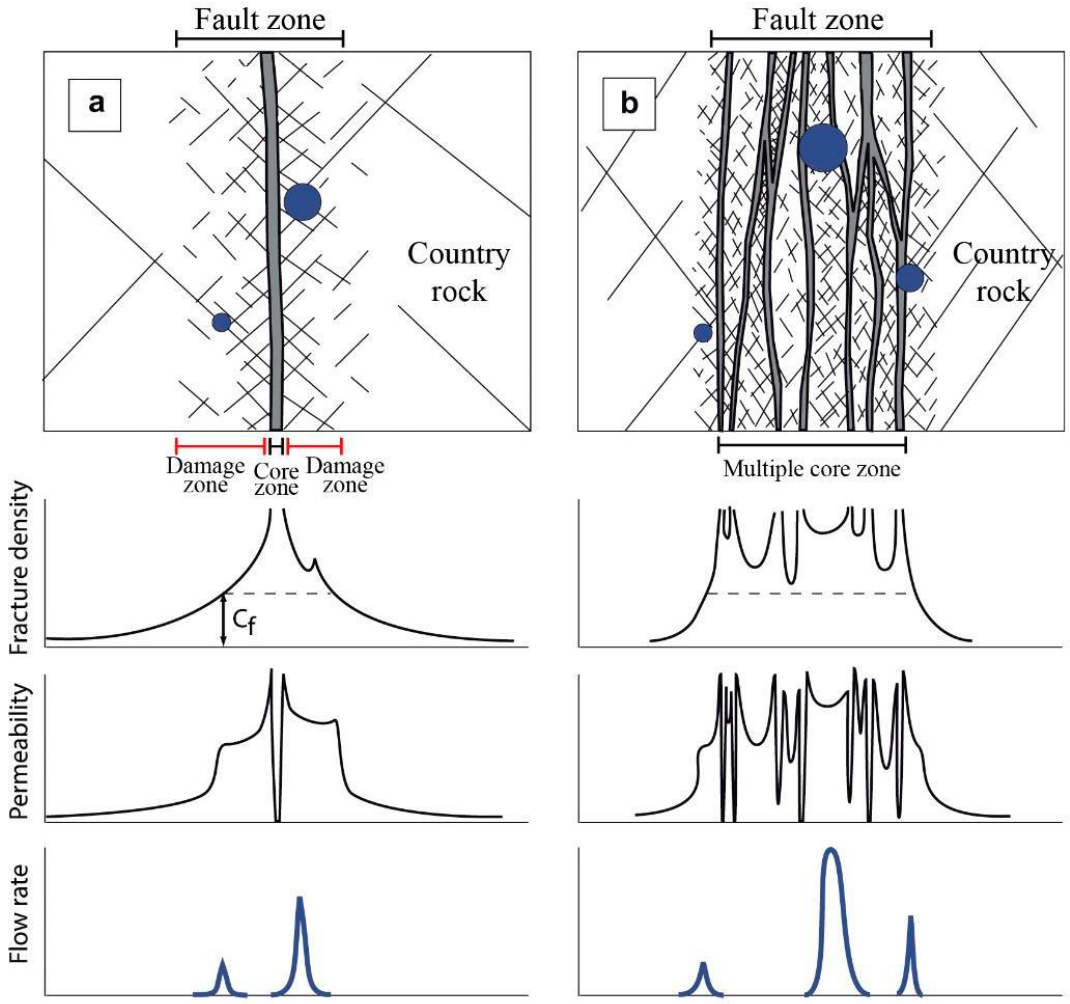

Figure 1: Simplified model of a fault zone and its relationship with fluid flow around the fault. Top charts represent conceptual architecture of the fault zone, consisting of a a) simple or b) multiple core zone, both surrounded by damage zone and protolith (country rocks). Blue dots represent high hydraulic conductivity zones. Graphs down show fracture density, permeability and flow rate variations according to the fault zone architecture (Modified from Faulkner et al., 2010 and Seebeck et al., 2014).

However, a usually open question that requires rather attention is what the exact control of fault zones on past and present fluid flow is. Several processes accompanying the failure of rock mass, such as cyclic ruptures on the same fault zone, mineral precipitation from fluids in veins, and dissolution of minerals in the vicinity of a fracture, promote a time-depending and enhancing/reducing fault controlled permeability. Numerous natural examples show successive paleo-fluid circulations in the same deformation zone, evidenced by overprinted hydrothermal mineralization and re-opening texture of veins related to its seismic period (e.g. Le Garzic et al. 2011; Bons et al., 2012). Moreover, considering the high sensitivity of the fault system regarding the rupture under prevailing stress and/or fluid overpressure conditions, estimation of permeability architecture of fault zone is widely studied but poorly constrained (e.g. Faulkner et al., 2010; Caine et al., 2010). This topic is becoming critical in the case of fluid flow into intrinsic low porosity/permeability crystalline rocks, where fault-related (or structural) permeability provides the main hydraulic conductivity. This condition could originate “fractured reservoirs” and examples include oil, gas, groundwater, and geothermal reservoirs (e.g. Nelson, 2001; Cox et al., 2001). In particular, numerous examples in the world have described and modelled the fault-controlled geothermal systems (e.g. Giordano et al., 2012; Vignaroli et al., 2013; Brehme et al., 2016; Wilson and Rowland, 2016).

To better understanding of present fluid flow, evidences of past fluid flow give a good information about long-term processes. In this work, we studied a tectonically active zone in Southern Chile and present preliminary results about its tectonic and structural nature, by strain analysis of inverted fault-slip data.

2. CASE OF STUDY

The Southern Andes volcanic zone (SVZ) provides one of the best natural laboratories to address the control of fault–fracture networks on geothermal systems. Previous work has been done about the occurrence of numerous geothermal areas (25% of Chilean thermal springs areas), active regional fault systems, and highly active volcanism resulted from the current tectonic setting (e.g. Stern, 2004; Haberland et al., 2006; Lange et al., 2008; Cembrano and Lara, 2009; Moreno et al. 2010; Legrand et al., 2011;

Sánchez et al., 2013; Aravena et al., 2016). Tectonic activity is represented by two active long-lived regional scale fault systems (Fig. 2a): the arc-parallel Liquiñe–Ofqui fault system (LOFS) and NW-striking Andean Transverse Faults (ATF), which have different tectonic domains (e.g. Cembrano et al., 1996; Rosenau et al., 2006; Melnick et al., 2006; Cembrano and Lara 2009; Sánchez et al., 2013; Sánchez et al., 2016; Pérez-Flores et al., 2016). (1) The LOFS domain, with NNE-striking master faults favorably orientated for dextral shear with respect to the prevailing stress field (e.g. σ1~N60E; Lavenu and Cembrano 1999; Rosenau et al., 2006) and NE-striking tension fractures likely to form under relatively low differential stress (e.g. Pérez-Flores et al., 2016). Volcanic activity comprises NE-trending volcanic alignments containing mainly basaltic to basaltic– andesitic lithologies in either stratovolcanoes or minor eruptive centres. Osorno–Puntiagudo–Cordon Cenizos volcanic alignment (located at 41°S) is an example of this type (e.g. Cembrano and Lara, 2009). (2) The ATF domain with WNW-striking faults severely misorientated with respect to the prevailing stress field (e.g. Pérez-Flores et al., 2016). The volcanic activity comprises WNW-striking alignments of stratovolcanoes and displays a more evolved magma series (basaltic to rhyolitic), providing the suitable conditions for the development of magma reservoirs and magma differentiation (e.g. Cembrano and Lara, 2009). One example is Tolhuaca volcano (38°18'S) and its Tolhuaca high-enthalpy geothermal system (explored but not yet exploited) which is characterized by several surficial thermal manifestations including areas with fumaroles, boiling pool and hot springs (e.g. Sanchez et al., 2016; Aravena et al., 2016).

At the northern part of LOFS (38°-39°S, Fig. 2a), recent studies (e.g. Sánchez et al., 2013; Sánchez et al., 2016; Pérez-Flores et al., 2016; Tardani et al., 2016) suggest that in the damage zone of strike-slip LOFS domain the vertical permeability is enhanced and deep convection occurs favored by the well-oriented fault–fracture networking. In contrast, ATZ have been interpreted as crustal weakness associated with pre-Andean faults reactivated as sinistral-reserve strike slip faults during arc development (e.g. Melnick et al., 2009). In this context, ATZ provides suitable conditions for the development of a hydrothermal reservoir controlling heat transfer mechanisms, where structural permeability is only enhanced under fluid overpressure conditions (Sanchez et al., 2016; Roquer et al., 2017). Immediately to South (39°S), a major NW-trending alignment is given by Villarrica-Quetrupillan-Lanin volcanoes spatially related to the presumably pre-Andean Mocha-Villarrica fault zone (MVFZ) (Fig. 2), striking from Chilean costal cordillera until Argentinian basins crossing the Andean cordillera (e.g. Rapela and Pankhurst, 1992; Zaffarana et al., 2010). This feature is the most relevant ATZ category structure of the zone, including major changes in the country rocks that they cut. In the northernmost part of the Villarrica volcano, they are mainly Miocene volcano-sedimentary crop out (e.g. Curamallín Formation), whereas southward, country rocks predominantly are granodiorites and tonalites of Cretaceous to Miocene age, part of the North Patagonian Batholith (NPB) (Fig. 2b) (e.g. Hervé, 1994).

For this work, we have chosen Liquiñe area (39°S) as case study, where both categories of volcano–tectonic domains previously described (LOFS and ATZ) are present, and where there is a high density spatially associated hot springs manifestations (Fig. 2b) (e.g. Sánchez et al. 2013; Tardani et al., 2016; Wrage et al., 2017). In this area, some hot springs upwelling of rocks such as glacial or fluvial deposits overlying granitoides or volcanic units and others directly from fractured granitic rocks (Sánchez et al., 2013; Tardani et al., 2016; Held et al., 2018). Recent geochemical data reveal the small-scale circulation of low-temperature fluids in a potential reservoir, resulting presumably from the presence of interconnected fault and fracture zones. A preliminary estimation of reservoir temperatures varies from 120-160°C suggesting a low- to medium-enthalpy geothermal system (Sánchez et al., 2013; Tardani et al., 2016; Held et al., 2017; Wrage et al., 2017). Magnetotelluric study in the area suggests that LOFS can be described as a deep sub-vertical narrow conductor, despite the non-occurrence of high temperature geothermal manifestations (Held et al., 2018). Structural, geochemical, and geophysical data are consistent with fault-controlled occurrence of hot springs into a fractured system, with a local small-scale circulation pattern along the main fault.

3. METHODS

With the objective of determining the strain patterns in the study area, we selected a representative fault exposure corresponding to the LOFS and the ATF (hereafter referred to as Los Añiques and Cachim structural sites, respectively). The strain analysis involved the description of the geometry, kinematics, textures and cross-cutting relationships of different faults, classified in terms of their internal texture. We registered the dimensions and orientations of the fault plane, the rake of the striation, and the sense of movement, as inferred from brittle kinematic indicators defined by Petit (1987). In this study, 70 faults were measured in Los Añiques and 44 faults were measured in Cachim.

To perform the strain analysis, we used the software Faultkin 8.0.7 (Marrett and Allmendinger, 1990; Allmendinger et al., 2012). The method is based upon two fundamental ideas: 1) the shear stress resolved from the traction acting during failure is parallel to the striation mark; 2) the maximum and minimum principal strain axes, i.e. the shortening-axis (P) and the extension-axis (T), lie within the plane defined by the striation mark and the pole to the fault plane (movement plane). In this manner, it is assumed that within the movement plane both the P- and T-axes lie at 45º from the pole-to-fault, in an arrangement kinematically consistent with the registered sense of slip.

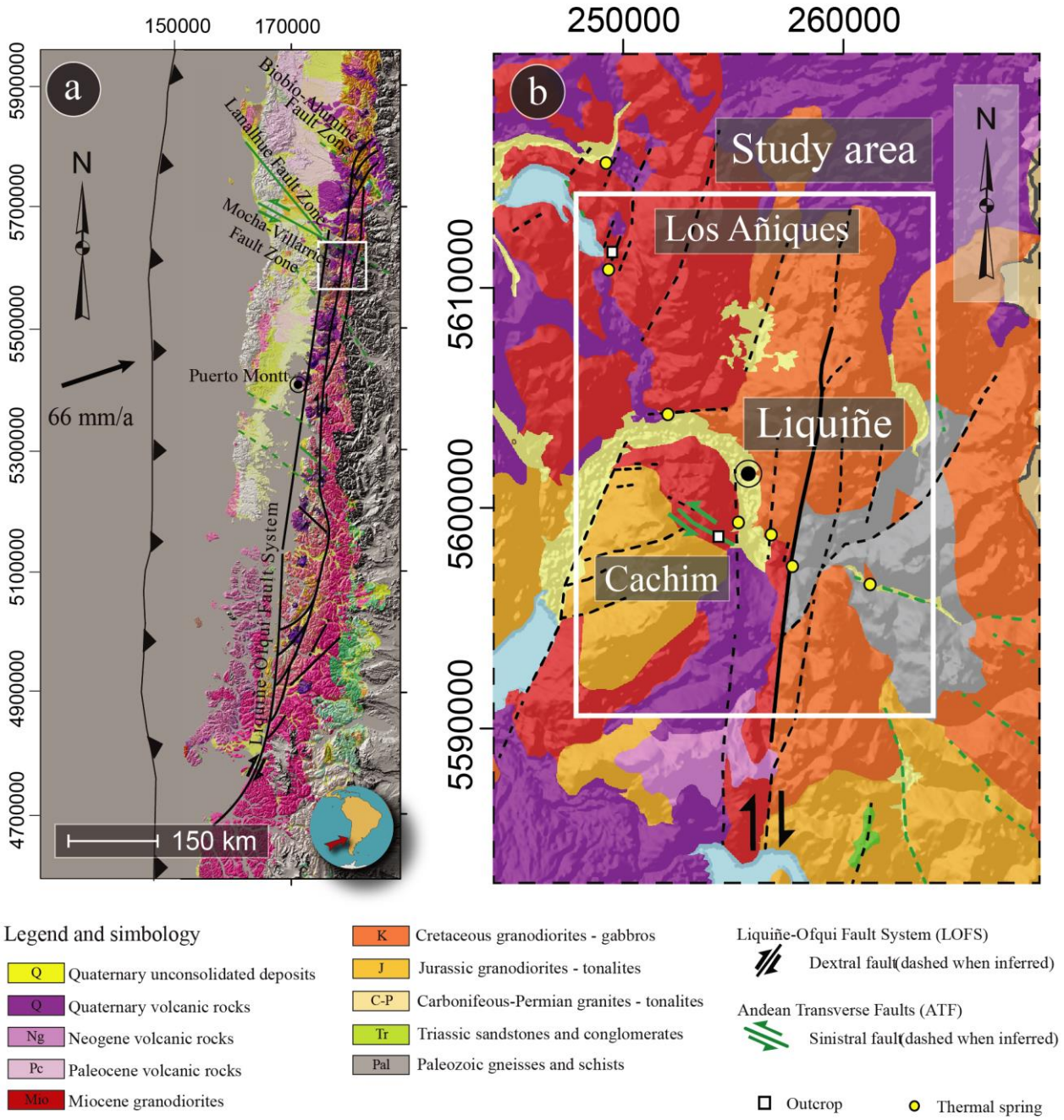

Figure 2: a) Tectonic framework of the Southern Volcanic Zone of the Andes (SVZ) (33°S-46°S). Tectonics of the SVZ is controlled by the Liquiñe-Ofqui Fault System (black lines) and the Andean Transverse Faults (green lines). b) Local geological context of the study area. The studied exposures are located on the white rectangle. Modified from Lara and Moreno (2004), Rosenau et al. (2006) and Sánchez et al. (2013).

The orientations of the P- and T-axes for each data plane were obtained, and different tectonic solutions were discriminated by distinguishing clusters of principal strain axes. Then, we obtained the best-fit Bingham distribution defining the identified clusters, and used σ-constructed contour intervals to assess the validity of the solution (e.g. Marrett and Allmendinger, 1990). Additionally, the strain tensor shape ratio R was calculated, using expression [1]:

$$R = \frac{E_2 - E_3}{E_1 - E_3} \quad [1]$$

Where E_1, E_2 and E_3 are the eigenvalues of the Bingham moment tensor the T, B (intermediate axis) and P-axes respectively (Allmendinger et al., 2012). Finally, R-values were interpreted in terms of the strain regime they define, indicating a constrictional regime for R= 0.00-0.35, a plane strain regime for R=0.35-0.65 and a flattening regime for R=0.65-1.00.

4. RESULTS

4.1 Faults within the structural sites

Structural mapping was carried out in two structural sites: Los Añiques and Cachim (Fig. 2b). Los Añiques site is spatially related to LOFS regional faults, whereas Cachim site is spatially associated with ATF system (Fig. 2b). For these cases, the most predominant kinematic indicators are steps and R surfaces.

In Los Añiques faults are exposed in patches of tens of square centimeters (Figs. 3a and b). Host rock is a Miocene granodiorite (Lara and Moreno, 2004). Faults are separated in three main groups according with their kinematics and orientations in: a) dextral normal and dextral reverse striking between N20ºE to N30ºE, dipping between 65º to 85º E and the rake is 10º to 50º preferentially to the S; b) sinistral reverse and sinistral normal, striking N20ºW to N70ºW, dipping to 50º to 80º to S and the rake is 05º to 10º and 20º to 50º to the S; c) sinistral reverse and sinistral normal striking between N70ºW and N70ºE, dipping between 50º to 85º to S, rake is 10º to 50º to E and W.

On the other hand, in Cachim structural site, faults are exposed in different patches of several tens of square centimeters, cutting both Miocene granodioritic host rock and andesitic dykes (Figs. 3c and d). In terms of their kinematics and orientations, faults in this outcrop are separated in three main groups: a) sinistral-reverse and dextral normal faults that strike N15-60ºW, dip 40º to 85º mostly to the NE, and have rakes <35º preferentially from the E; b) dextral-normal faults striking N10ºE to N30ºE, dipping between 60º to 80º to the NW, and rake is <20º mostly to N; c) sinistral-reverse faults striking N45ºE to N75ºW, dip 50º to 85º to the S, the rake is <20º mostly to the SW.

4.2 Strain solutions from fault-slip data

Distribution of P and T-axes in Los Añiques structural site, evidence a heterogeneous deformation, defining two strain solution. Solution I includes a 67% of collected data (47 of the 70 fault-slip data) and solution II includes the remaining data corresponding to 33% of the data (23 of the 70 fault slip-data) (Fig. 4a). The strain solution I shows a cluster of P and T-axes, yielding a kinematic tensor with subhorizontal NE-trending shortening axis, and subhorizontal stretching axis with NW-trending. The strain tensor shape ratio is R=0.69. Faults conforming solution I are mainly NE dextral-normal and dextral-reverse faults, NW to WNW sinistral-reverse faults. Solution II shows a cluster of P and T-axes, yielding a kinematic tensor with subhorizontal NW-trending shortening axis, and subhorizontal NE-trending stretching axis. The strain tensor shape ratio is R=0.40 and compatible faults with this solution are mainly NE dextral-reverse, ENE dextral-normal faults and NW sinistral-normal and sinistral dextral.

Deformation patterns derived from distribution of P and T-axes in the Cachim structural site, reveal heterogeneous deformation expressed as two strain solutions. Solution I is defined by 43% of the data (19 of the 44 fault-slip data), and solution II including the remaining 57% of the data (25 of the 44 fault-slip data) (Fig. 4b). Solution I shows well clustered distribution of the P and T-axes, defining a kinematic tensor with ENE-trending, subhorizontal shortening and NNW-trending, subhorizontal stretching axes. The strain tensor shape ratio of the solution is R=0.50. Faults defining solution I are NW sinistral-reverse faults and NE dextral-normal faults. Strain solution II also shows a well-defined distribution of the T and P-axes, presenting a kinematic tensor with and NS-trending, subhorizontal shortening axis, and the stretching axis is subhorizontal EW-trending. The strain tensor shape ratio is R_I=0.51 and faults defining solution II are NW dextral-normal and dextral-reverse and sinistral reverse that strike NE to ENE.

5. DISCUSSION AND CONCLUSION

For the cases of Los Añiques (LOFS exposure) and Cachim (ATF exposure) structural sites, strain analysis of fault-slip data shows bimodal distribution of the orientations of the P- and T-axes, in two tectonic solutions (solutions I and II). The proposed solutions and associated kinematic models are depicted in Fig. 5.

In Los Añiques structural site (LOFS exposure), solution I defines an ENE-trending, subhorizontal P-axis and a NNW-trending, subhorizontal T-axis (Fig. 5a). Eigenvalues of the fitted Bingham distribution indicate a strain tensor shape ratio R=0.69. From this follows that the value of the intermediate strain axis B ranges from a value of approximately equidistant magnitude to the P- and T-axes, to similar in magnitude to the P-axis. Therefore, in this tectonic regime, deformation ranges from plane strain to flattening strain ellipsoid (Marret and Allmendinger, 1990). Faults in this regime are mainly NNE-to-ENE striking sinistral-reverse faults, and NNE striking dextral-reverse and dextral-normal faults. On the other hand, solution II shows a NW trending, subhorizontal P-axis and a NNE-trending, subhorizontal T-axis (Fig. 5a). Eigenvalues of the best-fitted Bingham distribution indicate a strain tensor shape ratio R=0.40. From this follows that the value of B-axis has a value equidistant in magnitude to the P- and T-axes. In this manner, tectonic solution II defines a plane strain ellipsoid (Marret and Allmendinger, 1990). Faults in this solution are mostly NE-to-ENE striking sinistral-reverse and sinistral-normal faults, and NW striking dextral-reverse and dextral-normal faults (Fig. 5a).

Figure 3: Structural sites chosen for this study. a) Los Añiques structural site is related to LOFS exposure (strike of regional fault N30ºE). b) Example of fault in Los Añiques structural site; c) Cachim structural site is related to ATF exposure (strike of regional fault N70°W). d) Example of fault in Cachim structural site.

In Cachim structural site (ATF exposure), solution I defines an EW-trending, subhorizontal P-axis and a NS-trending, subhorizontal T-axis (Fig. 5b). Eigenvalues of the obtained Bingham distribution show a strain tensor shape ratio R=0.50. From this follows that the value of the intermediate strain axis B ranges from is of approximately equidistant magnitude to the P- and T-axes. Therefore, in this tectonic solution, plane strain-type deformation can be inferred (Marret and Allmendinger, 1990). Faults in this regime are mainly NE-to-ENE striking sinistral-reverse faults. On the other hand, solution II shows a NS trending, subhorizontal P-axis and an EW-trending, subhorizontal T-axis (Fig. 5a). Eigenvalues of the best-fitted Bingham distribution indicate a strain tensor shape ratio R=0.51. From this follows that the value of B-axis has a value equidistant in magnitude to the P- and T-axes. In this manner, tectonic solution II defines a plane strain ellipsoid (Marret and Allmendinger, 1990). Faults in this solution are mostly NNW-to-NW striking dextral-normal faults, and WNW striking sinistral-reverse faults (Fig. 5b).

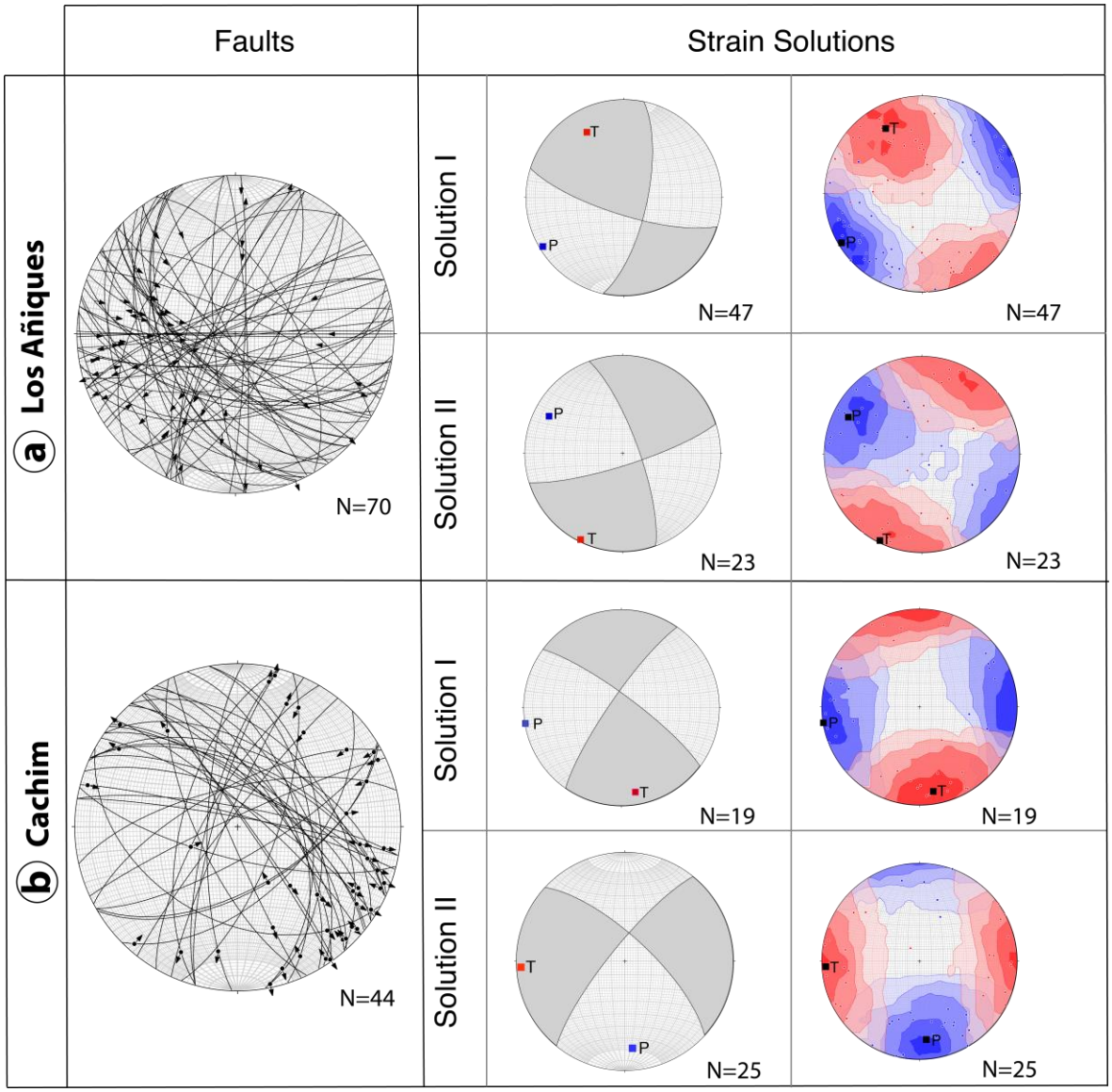

Figure 4: Fault-slip data and strain solutions of a) Los Añiques and b) Cachim structural sites. Stereograms show lower hemisphere, equal area projections of (from left to right): fault-slip data (direction of the hanging wall block is indicated in the triangles); obtained tectonic strain solution, and individual maximum (P, blue) and minimum (T, red) principal strain axes.

Solution I, in both Los Añiques (LOFS exposure) and Cachim (ATF exposure) structural sites, show orientations of the principal strain axes that are in good agreement with tectonic solutions arising from partially partitioned strain due to oblique plate convergence, which shape intra-arc long-term stress conditions of the Southern Volcanic Zone of the Andes (e.g. Teyssier et al., 1995; Rosenau et al., 2006; Pérez-Flores et al., 2016; Stanton-Yonge et al., 2016; Sielfeld et al., 2019). This follows because bulk strike-slip transpressional deformation partitions into NS-to-ENE striking faults of the LOFS, which accommodate a NE-to-ENE trending P-axis, and into NW-to-WNW striking faults of the ATF, which would accommodate a WNW-to-EW trending P-axis (e.g. Pérez-Flores et al., 2016). Moreover, kinematics of the regional faults, which would be defined by the geometry of regional lineaments and orientation and shape of the strain ellipsoid, is consistent with long-term kinematic behavior of the LOFS and ATF. Los Añiques structural site (LOFS exposure) would represent a N30ºE-striking dextral regional fault, whereas Cachim structural site (ATF exposure) would represent a N70ºW-striking, sinistral regional fault.

On the other hand, solution II in both Los Añiques (LOFS exposure) and Cachim (ATF exposure) structural sites seem to be decoupled from long-term stress conditions of the study area. Decoupled tectonic solutions of the LOFS and the ATF might be related to (e.g. Hardebeck, 2012; Rosenau et al., 2006; Stanton-Yonge et al., 2016): 1) sporadic changes in crustal regional stress as a result of continental plate relaxation during the co-postseismic phases of the Andean subduction cycle 2) decoupling from crustal regional strain due to variations in local strain conditions. In the first case, these tectonic solutions could be associated to a regional state of stress, in which decoupled solutions would yield a kinematic variation of regional faults. This means that Los Añiques structural site (LOFS exposure) would represent a N30ºE-striking compressional fault, whereas Cachim structural site (ATF exposure) would represent a N70ºW-striking, dextral fault.

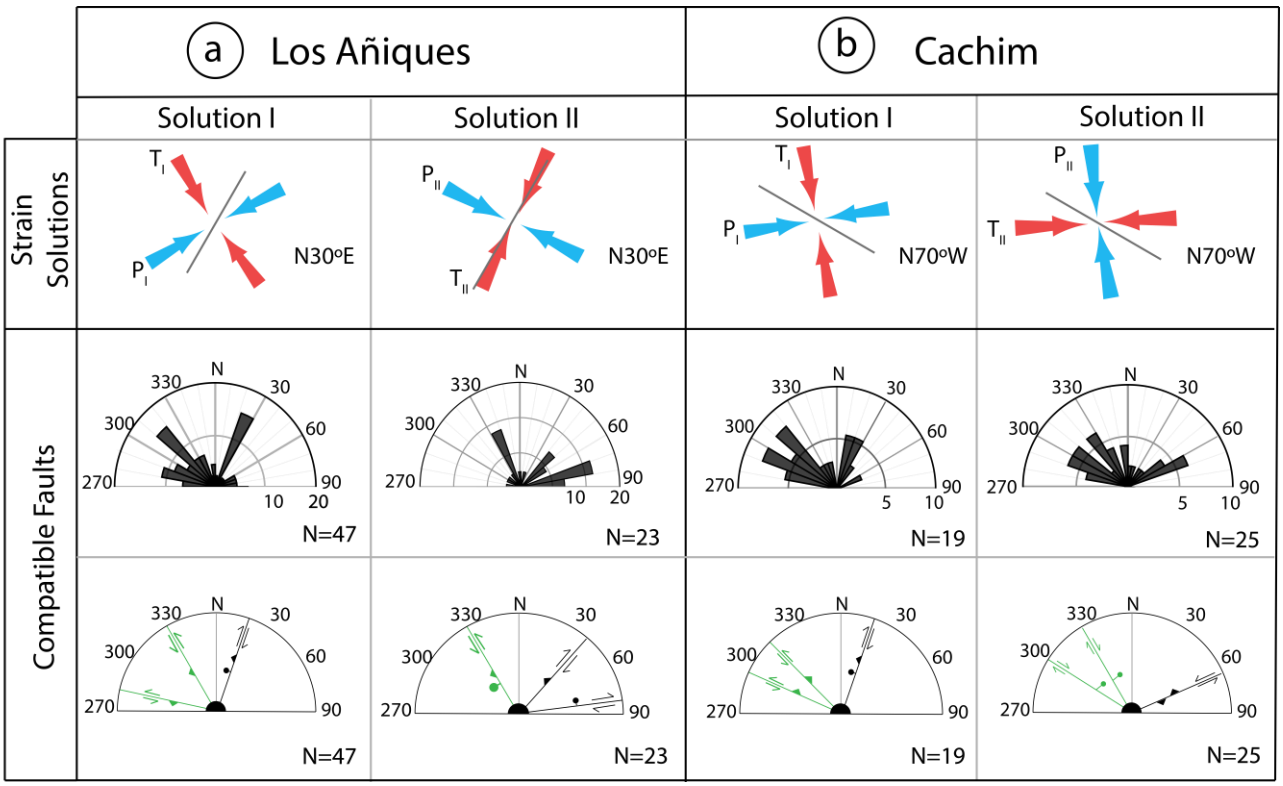

Figure 5: Proposed kinematic model for a) Los Añiques (LOFS) and b) Cachim (ATF) structural sites. Above, schematic representation of proposed strain solutions (plan view): maximum principal strain axe (P) = blue; minimum principal strain axe (T) = red. Main regional N30°E-trending and N70°W-trending lineaments, were identified in Los Añiques and Cachim sites, respectively. Center: rose diagrams for the faults compatible with each strain tectonic solution. Below: schematic representation of the main behavior for the compatible faults.

In conclusion, from the data presented here, we hypothesize that fault-driven structural permeability may occur within fault-vein meshes associated with regional faults, at specific orientations as given strain tectonic solutions (e.g. Sibson, 1994). This means that hydrostructural conditions in the Liquiñe area are governed by varying kinematic conditions, rather than by homogeneous strain.

ACKNOWLEDGEMENTS

This work is a contribution to the FONDECYT project #1180167 and the FONDAP/CONICYT project #15090013 “Centro de Excelencia en Geotermia de los Andes” (CEGA). TR acknowledges financial support from CONICYT PhD grant #21171178.

REFERENCES

1. Allmendinger, R. W., Cardozo, N. C., and Fisher, D. 2012. Structural Geology Algorithms: Vectors & Tensors: Cambridge, England, *Cambridge University Press*, 289 pp.
2. Aravena, D., Muñoz, M., Morata, D., Lahsen, A., Parada, M.A., Dobson, P. 2016. Assessment of high enthalpy geothermal resources and promising areas of Chile. Geothermics 59, 1–13.
3. Bons, P.D., Elburg, M.A., Gomez-Rivas, E., 2012. A review of the formation of tectonic veins and their microstructures. J. Struct. Geol. 43, 33-62.
4. Brehme M., Blöchera G., Cacacea M., Deona, F., Moeck, I., Wiegandb, B., Kamahc Y., Regenspurga S., Zimmermann, G, Sauterb M, Huengesa, E. 2016. Characterizing permeability structures in geothermal reservoirs – A case study in Lahendong. PROCEEDINGS, 41st Workshop on Geothermal Reservoir Engineering Stanford University, Stanford.
5. Bons, P.D., Elburg, M.A., Gomez-Rivas, E., 2012. A review of the formation of tectonic veins and their microstructures. J. Struct. Geol. 43, 33-62.
6. Caine, J.S., Bruhn, R.L., Forster, C.B., 2010. Internal structure, fault rocks, and inferences regarding deformation, fluid flow, and mineralization in the seismogenic stillwater normal fault, Dixie Valley, Nevada. J. Struct. Geol. 32, 1576-1589.
7. Cembrano, J., Herve, F. Lavenu, A. 1996. The Liquiñe-Ofqui Fault Zone: a long-lived intra-arc fault system in southern Chile. Tectonophysics 256, 55-66.
8. Cembrano, J., Schermer, E., Lavenu, A., and Sanhueza, A. 2000. Contrasting nature of deformation along an intra-arc shear zone, the Liquiñe–Ofqui fault zone, southern Chilean Andes. Tectonophysics, 319(2), 129-149.
9. Cembrano, J., and Lara, L.E. 2009. The link between volcanism and tectonics in the southern volcanic zone of the Chilean Andes: A review: Tectonophysics 471, 96–113.
10. Cox, S.F., Knackstedt, M.A., Marini, L., Raco, B. 2001. Principles of structural controls on permeability and fluid flow in hydrothermal systems. Rev. Econ. Geol. 14, 1-24.
11. Cox, S. 2010. The application of failure mode diagrams for exploring the roles of fluid pressure and stress states in controlling styles of fracture-controlled permeability enhancement in faults and shear zones. Geofluids 10, 217–233.
12. Faulkner,D., Jackson,C., Lunn, R., Schlische, R., Shipton, S., Wibberley, C., Withjack, M. 2010. A review of recent developments concerning the structure, mechanics and fluid flow properties of fault zones. J. Struct. Geol. 32, 1557-1575.

13. Giordano, G., Pinton, A., Cianfarra, P., Baez, W., Chiodi, A., Viramonte, J., Norini, G., Groppelli, G. 2012. Structural control on geothermal circulation in the Cerro Tuzgle-Tocomar geothermal volcanic area (Puna plateau, Argentina). J. Volcanol. Geotherm. Res. 249, 77-94.
14. Gudmundsson, A. 2011. Rock fractures in geological process. First Edition, Cambridge University Press, UK, ISBN 978-0-521-86392-6, 578 p.
15. Haberland, C.C., Rietbrock, A., Lange, D., Bataille, K., Hofmann, S., 2006. Interaction between forearc and oceanic plate at the south-central Chilean margin as seen in local seismic data. Geophys. Res. Lett. 33, 1-5.
16. Hardebeck, J. L. 2012. Coseismic and postseismic stress rotations due to great subduction zone earthquakes. Geophysical Research Letters, 39(21).
17. Held, S., Schill, E., Schneider, J., Nitschke, F., Morata, D., Neumann, T., Kohl, T. 2018. Geochemical characterization of the geothermal system at Villarrica volcano, Southern Chile; Part 1: Impacts of lithology on the geothermal reservoir. Geothermics 74, 226-239.
18. Hervé, F. 1994. The Southern Andes Between 39° and 44°S Latitude: The Geological Signature of a Transpressive Tectonic Regime Related to a Magmatic Arc, in: Tectonics of the Southern Central Andes, 243–248.
19. Lange, D., Cembrano, J., Rietbrock, a., Haberland, C., Dahm, T., Bataille, K., 2008. First seismic record for intra-arc strike-slip tectonics along the Liquiñe-Ofqui fault zone at the obliquely convergent plate margin of the southern Andes. Tectonophysics 455, 14–24.
20. Lara, L., Moreno, H. 2004. Geología del Área Liquiñe-Neltume, Regiones de Los Lagos y de la Araucanía. Servicio Nacional de Geología y Minería. Carta Geológica de Chile, Serie Geología Básica, 83, 1. Scale 1:100.000.
21. Lavenu, A., Cembrano, J., 1999. Compressional- and transpressional-stress pattern for Pliocene and Quaternary brittle deformation in fore arc and intra-arc zones (Andes of Central and Southern Chile). J. Struct. Geol. 21, 1669–1691.
22. Le Garzic, E., De L'Hamaide, T., Diraison, M., Champanhet, J. 2011. Scaling and geometric properties of fracture systems in Proterozoic basement of Yemen (Al Mukalla area). Tectonic interpretation and fluid flow implications. J. Struct. Geol. 33, 519-536.
23. Legrand, D., Barrientos, S., Bataille, K., Cembrano, J., Pavez, A., 2011. The fluid-driven tectonic swarm of Aysen Fjord, Chile (2007) associated with two earthquakes (Mw=6.1 and Mw=6.2) within the Liquiñe-Ofqui Fault Zone. Cont. Shelf Res. 31, 154–161.
24. Marrett, R., Allmendinger, R.W., 1990. Kinematic analysis of fault-slip data. J. Struct. Geol. 12(8), 973–986.
25. Melnick, D., Rosenau, M., Folguera, A., Echtler, H., 2006. Neogene tectonic evolution of the Neuquén Andes western flank (37-39°S). Geol. Soc. Spec. Pap. 407.
26. Melnick, D., Bookhagen, B., Strecker, M.R., Echtler, H.P., 2009. Segmentation of megathrust rupture zones from forearc deformation patterns over hundreds to millions of years, Arauco peninsula, Chile. J. Geophys. Res. 114, B01407.
27. Mickelthwaite, S., Sheldon, H., Baker, T. 2010. Active fault and shear processes and their implications for mineral deposit formation and discovery. J. Struct. Geol. 32, 151-165.
28. Moreno, M., Rosenau, M., Oncken, O. 2010. Maule earthquake slip correlates with pre-seismic locking of Andean subduction zone. Nature 467, 198–202.
29. Nelson, R.A. 2001. Geologic Analysis of Naturally Fractured Reservoirs. 2nd Edition. Gulf Professional Publishing, Butterworth–Heinemann, ISBN 0-88415-317-7, 332 p.
30. Petit, J. P. 1987. Criteria for the sense of movement on fault surfaces in brittle rocks. Journal of Structural Geology, 9(5-6), 597-608.
31. Pérez-Flores, P., Cembrano, J., Sanchez, P., Veloso, E., Arancibia, G., Roquer, T. 2016. Tectonics, magmatism and paleo-fluid distribution in a strike-slip setting: Insights from the northern termination of the Liquiñe-Ofqui fault System, Chile. Tectonophysics, 192-210.
32. Rapela, C.W., Pankhurst, R.J. 1992. The granites of northern Patagonia and the Gastre Fault System in relation to the break-up of Gondwana: Geological Society, London, Special Publications 68 (1), 209–220.
33. Rosenau, M., Melnick, D., Echtler, H., 2006. Kinematic constraints on intra-arc shear and strain partitioning in the southern Andes between 38°S and 42°S latitude. Tectonics 25, 1-16.
34. Roquer, T., Arancibia, G., Rowland, J., Iturrieta, P., Morata, D., Cembrano, J. 2017. Fault-controlled development of shallow hydrothermal systems: structural and mineralogical insights from the Southern Andes. Geothermics 66, 156-173.
35. Rowland, J.V., Sibson, R.H. 2004. Structural controls on hydrothermal flow in a segmented rift system, Taupo Volcanic Zone, New Zealand. Geofluids 4, 259-283.
36. Sánchez, P., Pérez-Flores, P., Arancibia, G., Cembrano, J., Reich, M. 2013. Crustal deformation effects on the chemical evolution of geothermal systems: the intra-arc Liquiñe–Ofqui fault system, Southern Andes. Int. Geol. Rev. 55 (11), 1384–1400.
37. Sánchez-Alfaro, P., Reich, M., Arancibia, G., Pérez-Flores, P., Cembrano, J., Driesner, T., Lizama, M., Rowland, J., Morata, D., Heinrich, C., Tardani, D., Campos, E. 2016. Physical, chemical and mineralogical evolution of the Tolhuaca geothermal system, southern Andes, Chile: insights into the interplay between hydrothermal alteration and brittle deformation. J. Volcanol. Geotherm. Res., 88-104.
38. Stern, C.R. 2004. Active Andean volcanism: its geologic and tectonic setting: Andean Geology 31 (2), 161– 206.
39. Seebeck H, Nicol A, Walsh JJ, Childs C, Beetham RD, Pettinga J. 2014. Fluid flow in fault zones from an active rift. J. Struct. Geol. 62, 52-64.
40. Sibson, R.H. 1994. Crustal stress, faulting and fluid flow. Geological Society, London, Special Publications, 78(1), 69-84.
41. Sibson, R.H. 2001. Seismogenic framework for hydrothermal transport and ore deposition. Rev. Econ. Geol. 14, 25-50.
42. Sielfeld, G., Lange, D., Cembrano, J. 2019. Intra-Arc Crustal Seismicity: Seismotectonic Implications for the Southern Andes Volcanic Zone, Chile. Tectonics, *in press*, https://doi.org/10.1029/2018TC004985
43. Stanton-Yonge, A., Griffith, W. A., Cembrano, J., St. Julien, R. and Iturrieta, P. 2016. Tectonic role of margin-parallel and margin-transverse faults during oblique subduction in the Southern Volcanic Zone of the Andes: Insights from Boundary Element Modeling. Tectonics, 35(9), 1990-2013.
44. Teyssier, C., Tikoff, B., Markley, M. 1995. Oblique plate motion and continental tectonics. *Geology*, 23(5), 447-450.

45. Tardani, D., Reich, M., Roulleau, E., Takahata, N., Sano, Y., Pérez-Flores, P., Sánchez, P., Cembrano, J., Arancibia, G. 2016. Exploring the structural controls on helium, nitrogen and carbon isotopes composition in hydrothermal fluids along an intra-arc fault system. Geoch. Cosmochim. Acta, 193-211.
46. Vignaroli, G., Pinton, A., De Benedetti, A., Giordano, G., Rossetti, F., Soligo, M., Berardi, G. 2013. Structural compartmentalization of a geothermal system, the Torre Alfina field (central Italy). Tectonophysics 608, 482-498.
47. Wilson, C., Rowland, J. 2016. The volcanic, magmatic, and tectonic setting of the Taupo Volcanic Zone, New Zealand, reviewed from a geothermal perspective. Geothermics 59, 168-187.
48. Wrage, J., Tardani, D., Reich, M., Daniele, L., Arancibia, G., Cembrano, J., Sánchez-Alfaro, P., Morata, D. 2017. Geochemistry of thermal waters in the Southern Volcanic Zone, Chile- Implications for structural controls on geothermal fluid composition. Chemical Geology 466: 545-561.
49. Zaffarana, C.B., López de Luchi, M.G., Somoza, R., Mercader, R., Giacosa, R., and Martino, R.D., 2010, Anisotropy of magnetic susceptibility study in two classical localities of the Gastre Fault System, central Patagonia: J. South Am. Earth Sc. 30 (3-4), 151–166.